Composites Science and Technology xxx (2008) xxx–xxx

Contents lists available at ScienceDirect

Composites Science and Technology

journal homepage: www.elsevier.com/locate/compscitech

Shock loading response of sandwich panels with 3-D woven E-glass composite skins and stitched foam core

Srinivasan Arjun Tekalur [a], Alexander E. Bogdanovich [b], Arun Shukla [a,*]

[a] Dynamic Photomechanics Laboratory, University of Rhode Island, Kingston, RI 02881, USA
[b] 3TEX Inc., Cary, NC 27511, USA

ARTICLE INFO

Article history:
Received 10 October 2007
Received in revised form 5 March 2008
Accepted 13 March 2008
Available online xxxx

Keywords:
A. Structural composites
A. Glass fibers
C. Damage tolerance
C. Sandwich structures
Blast resistance

ABSTRACT

Sandwich composite are used in numerous structural applications, with demonstrated weight savings over conventional metals and solid composite materials. The increasing use of sandwich composites in defense structures, particularly those which may be exposed to shock loading, demands for a thorough understanding of their response to suc highly transient loadings. In order to fully utilize their potential in such extreme conditions, design optimization of the skin and core materials are desirable. The present study is performed for a novel type of sandwich material, TRANSONITE® made by pultrusion of 3-D woven 3WEAVE® E-glass fiber composites skin preforms integrally stitched to polyisocyanurate TRYMER™ 200L foam core. The effect of core stitching density on the transient response of three simply supported sandwich panels loaded in a shock tube is experimentally studied in this work. The experimental program is focused on recording dynamic transient response by high-speed camera and post-mortem evaluation of imparted damage. The obtained experimental results reveal new important features of the transient deformation, damage initiation and progression and final failure of sandwich composites with unstitched and stitched foam cores. The theoretical study includes full 3-D dynamic transient analysis of displacement, strain and stress fields under experimentally recorded surface shock pressure, performed with the use of 3-D MOSAIC analysis approach. The obtained theoretical and experimental results for the transient central deflections in unstitched and two stitched foam core sandwiches are mutually compared. The comparison results reveal large discrepancies in the case of unstitched sandwich, much smaller discrepancies in the case of intermediate stitching density, and excellent agreement between theoretical and experimental results for the sandwich with the highest stitching density. The general conclusion is that further comprehensive experimental and theoretical studies are required in order to get a thorough understanding of a very complex behavior of composite sandwiches under shock wave loading.

1. Introduction

Sandwich materials are utilized in the naval and aerospace industry for their weight saving and high specific strength advantages. The mechanical behavior and structural response of sandwich materials under quasi-static loadings were studied in earlier publications, see [1–3] among few references. Often, such sandwich structures are subjected to highly transient shock loading conditions, with the surface pressure spread over the entire structure or over a certain area. In the recent times, experimental studies of response of sandwich structures to such dynamic loadings have been reported in [4,5].

The overall dynamic response of the sandwich is dependent, among several other factors, on the construction of the skin, compressive and shear moduli and strengths of the core, and the interface bonding strength between the skin and core. Due to the inherent nature of its construction, the strength of the whole sandwich structure is often limited by the strength of the core material. The skin may also appear the weakest link, then its thickness may be increased, but if increased beyond certain limit, it would negate the weight advantage of sandwich structures. Thus, maximizing the strength of core, skin and the interface between them vs. simply increasing thickness (and, consequently, weight) of the skin and core, is a much better alternative.

In lieu of these considerations and with the aim of obtaining better dynamic performance under shock loading, several design advancements have been sought after. These include better choice of core material, introduction of soft inter-layers (e.g. polyurea layer) between the core and the skin, etc. Also, *Z*-directional pins have been utilized in [6] to modify the core and improve overall response of the sandwich to high strain rate impact loading. Authors of [7] studied failure modes of carbon fiber based sandwich beams reinforced with *Z*-directional pins under three-point bending.

* Corresponding author. Tel.: +1 401 874 2283; fax: +1 404 874 2355.
E-mail address: shuklaa@egr.uri.edu (A. Shukla).

0266-3538/$ - see front matter © 2008 Elsevier Ltd. All rights reserved.
doi:10.1016/j.compscitech.2008.03.017

The present study (it was initially reported in [5]) is focused on two new structural improvements of sandwich materials, namely, (1) superior skin construction by using 3-D woven fabric preforms for composites skins and (2) stiffening and strengthening the core and increasing its binding to the skins by through-thickness integral stitching of the skin preforms and foam core before resin infusion. This novel type of composite sandwich materials, named TRANSONITE®, is presently manufactured by Martin Marietta Composites by pultrusion method. One of its particular cases utilizes 3WEAVE® (three-dimensional orthogonal woven fabrics) manufactured by 3TEX for the skin reinforcement and TRYMER™ 200L foam as the core material. This type of sandwich has great potential for the applications where it is required to combine light-weight, high structural load-bearing capability, efficient blast mitigation ability, high damage tolerance and general survivability.

In the sandwich constructions used here, the 3-D woven skin preforms, made of E-glass roving, and the core were stitched together by a similar E-glass roving. The stitching pattern can be varied. Using higher stitching density results, firstly, in reduced through-thickness deformability of the core which, in turn, dramatically alternates the whole sandwich transient deformation mechanism. Secondly, through-thickness stitching of the skin preforms with the core substantially increases their interface strength and overall integrity of the sandwich structure, resulting in enhanced fracture toughness and damage tolerance. Thirdly, introducing transverse stitches to the core makes significant effect on its local stress–strain fields under transient loading.

Practical needs for 3-D dynamic structural analysis tools capable of accurately predicting the explosive blast effects on layered, composite, sandwich and other similar material types used in civil engineering, marine, ground vehicle, helicopter, aircraft, etc. structures, has grown tremendously in the last several years. In general, the required theoretical methods and analysis tools should address a number of specific practical problems. Among them are: (i) establishing relations between the "ideal" or "non-ideal" explosive characteristics on one side and the "field-free" blast pressure history on the other; (ii) correlating the field-free and the "true" pressure pulse acting on the structural elements like front wall, back wall, side wall, roof, ceiling, etc. Typical structural materials are highly vulnerable to blast overpressure even if exposed to a rather low-mass explosive charges at a relatively short standoff distances. Predecessors of total fracture and collapse of the structures exposed to blast overpressure are initiation and growth of cracks, their coalescence, followed by the material fragmentation, and spalling from the back surface. All of these phenomena occur during a very short, several millisecond time interval.

There are many analytical and computational approaches described in the literature, see [8–13] for example. They are aimed at solving the aforementioned scope of blast-related practical problems and range from rudimentary closed-form solutions to 3-D dynamic finite element packages like LS DYNA and ABAQUS. One quite simplistic finite element analysis approach, which is often used in blast response analysis of civil engineering structures is described in technical manual for Army [11]. It assumes that each building component responds as the equivalent single-degree-of-freedom system. This approach was also recommended in some of the later blast resistant structures design manuals [12,13].

In the above sources a blast pressure vs. time relationship is typically characterized by a peak pressure, impulse and shape. It is commonly assumed that the blast pressure rises instantaneously to its peak value, however under a more scrupulous look, the blast pressure rise stage may last for tens or even hundreds of microseconds. The second stage typically consists of a relatively long steady level pressure, followed by an even longer exponential decay to ambient pressure. Then there is a rather long time period when the pressure is below the ambient pressure. In the negative phase of the pressure history, the maximum pressure magnitude is typically small compared to the positive pressure magnitude and is commonly neglected in the analysis. Importantly, the so-called "reflected blast pressure" acting on the front wall may significantly exceed the peak field-free pressure. In the result of all these considerations, the incident pressure pulse can be reasonably represented by a "triangle-type" curve with the peak pressure multiplied by the "reflection factor" in the case of a front wall.

The above features of the blast pressure variation are well known and were mentioned here only with the aim to emphasize that in-depth understanding of the specifics of shock wave formation and adequate quantification of the entire pressure pulse history are crucial for a successful prediction of the respective transient structural response. Obviously, most sophisticated and accurate structural analysis tools would not provide useful results if the incident blast pressure is poorly defined. This statement also underscores how important it is to combine theoretical predictions of blast effects on practical structures with appropriate experimental studies. To these authors' best knowledge, first attempt to tie together theoretical and experimental studies of 3-D woven composites exposed to transient shock wave loading was made in [5], where theoretical results generated by 3TEX's in-house 3-D MOSAIC analysis tool were compared to some of experimental data presented in [14]. Experimental studies of the transient response of sandwich structures loaded in a shock wave tube [5] have not yet been tied to theoretical work. Such effort is undertaken in this paper.

The experimental method used here is similar to the method reported in [14], where several different 3-D woven fabric composites made of S-2 glass fiber and Derakane 8084 epoxy–vinyl ester resin were exposed to a highly transient dynamic loading in a shock tube. However, the object of present study is very different – instead of a one layer or two layer relatively thin solid composites we now have a thick sandwich panel with quite a complex construction and reinforcement architecture. Accordingly, the transient deformation, damage progression and failure phenomena are totally different than those observed in [14].

Regarding theoretical part of this work, the original 3TEX's in-house 3-D MOSAIC variational analysis approach and computer code are used here. The necessary mathematical details of this analysis approach and its various application examples can be found in [15–18]. The approach has totally different mathematical background than conventional 3-D hexahedral finite element and it provides significant analytical, algorithmical and computational advantages, see [15] for details. However, its objective is the same: to accurately predict 3-D static and dynamic stress–strain fields, damage, fracture and failure processes in complex composite material systems. The analysis approach is displacement-assumed; it employs Hamilton's variational principle with Bernstein approximation polynomials of an arbitrary degree used as the basis functions in all three coordinate directions. The displacement continuity is imposed between the layers. The interlaminar stress continuity conditions are satisfied with controlled accuracy as natural internal boundary conditions. Similarly, the external surface traction boundary conditions are satisfied in a "soft" variational sense with controlled accuracy.

In its dynamic version, see [16], 3-D MOSAIC analysis approach preserves all individual inertia terms without "lumping", thus allowing to study the whole variety of 3-D stress wave propagation processes. This may be especially important when analyzing those composites and sandwiches which contain very different constituent material densities (like foam core vs. E-glass composite) and geometric parameters (like skin thickness vs. core thickness). Damping (energy dissipation) factors can be also accounted in the analysis. Earlier applications of this analysis approach to the transient response predictions of thick layered panels composed

Please cite this article in press as: Tekalur SA et al., Shock loading response of sandwich panels with 3-D woven E-glass composite skins ..., Compos Sci Technol (2008), doi:10.1016/j.compscitech.2008.03.017

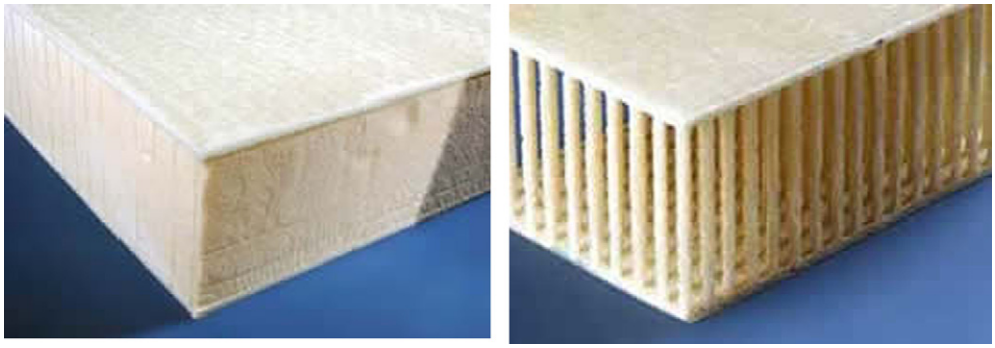

Fig. 1. TRANSONITE composite sandwich (left) and same with removed foam (right) as through-thickness "stitches", impregnated with resin, can be seen. Images borrowed from Martin Marietta Composites website.

from various materials (like polymer matrix composites, concrete, ceramics) were reported in [19,20].

2. Materials

2.1. Composite skins

Three-dimensional orthogonal woven preforms manufactured by 3TEX Inc., have the trademark 3WEAVE®. Their fabrication aspects and construction features can be found in a number of publications, see [20–23] for example; the latter paper also provides an extensive list of prior publications in this area.

The composite skin materials utilized in this study were made by VARTM method from 3.25 kg/m^2 (96 oz/yd^2) areal density 3WEAVE® E-glass glass roving preforms using Dow Derakane 8084 epoxy–vinyl ester resin. The fabric was manufactured from PPG Hybon 2022 E-glass roving in warp, fill and *Z*-directions; it contains three warp and four fill layers. Warp layers #1 and #3 use 218 yield roving, while layer #2 uses 450 yield roving. All warp layers have seven ends/in. (2.8 ends/cm) insertion frequency. All fill layers are made of 330 yield roving. The insertion frequency in fill direction is 6.7 picks/in. (2.6 picks/cm). *Z*-directional reinforcement uses 1800 yield roving with seven ends/in. (2.8 ends/cm) insertion frequency. This fabric construction results in ~49% warp-, ~49% fill- and ~2% *Z*-fiber content per preform volume. The total fiber volume fraction in a single layer composite made with such preform was estimated as ~49%.

In the previous work [14] four composite materials, made by VARTM with the use of four different S-2 glass fiber 3WEAVE® preforms, were experimentally studied under shock loading. One of these four preforms, having 3.15 kg/m^2 (93 oz/yd^2) areal density, is very similar in its fiber architecture to the above described 3.25 kg/m^2 areal density E-glass preform.

2.2. Foam core material

The core material used in the sandwich was made of Dow Chemical TRYMER™ 200L polyisocyanurate foam, which is a cellular polymer. This foam is specified to be ideal for applications in which a lightweight, low-density core is needed; the foam is less brittle than conventional polyisocyanurate foams. This foam is compatible with most thermoset resins, including vinyl esters and epoxies. From the manufacturer's data, the density of the foam is 32 kg/m^3. This foam is not an isotropic material; besides, its tensile and compressive properties are markedly different. Specifically, the foam manufacturer provides the following tensile, compressive and shear moduli in the direction parallel to rise: 8.27, 5.17 and 1.79 MPa, respectively. Its tensile (volumetrically averaged) compressive (parallel to rise) and shear (volumetrically average of parallel to rise and extruded directions) strengths are: 0.207, 0.207 and 0.159 MPa, respectively. The authors did not conduct their own testing of this standard Dow Chemical product.[1]

2.3. Sandwich fabrication and constructions

In all samples, the first two layers of the front skin (to be exposed to a shock wave) were made of the standard 0.81 kg/m^2 (24 oz/yd^2) areal density 2-D E-glass plain weave. Those were followed by three layers of 3WEAVE® fabric described in Section 2.1 and subsequently by a layer of foam core described in Section 2.2. The back skin preform contained (counting from the back surface of the core) two layers of the same 3WEAVE® fabric followed by two layers of the same E-glass plain weave. The front skin was intentionally made one fabric layer thicker than the back one, because other tests and theoretical analysis of this type of sandwich constructions, performed prior to this work, indicated that, if both skins have same thickness, the strains/stresses generated in the front skin are significantly higher and hence it had to be enhanced.

The work on fabricating TRANSONITE® sandwich panels, samples of which were used in this study, was performed by Martin Marietta Composites.[2] This sandwich type is produced in accordance with patented technology and provides an alternative for structural and non-structural flat panel applications. Delamination, which is a common problem in conventional sandwich materials, is virtually eliminated due to the through-thickness "stitches" (seen in Fig. 1). The stitches not only reinforce the foam core but also tie together layers of fabrics that make the skin preforms. From the viewpoint of through-thickness reinforcement, such stitches can be qualified as unidirectional composite bars impregnated by some polymeric resin.

A generic TRANSONITE® sandwich product shown in Fig. 1 is a pultruded assembly of a number of dry 2-D woven fabric layers and foam core in between. This assembly is first stitched on automated machine (in our case using 113 yield E-glass roving) with the chosen stitch density (in our samples it was 4 stitches/in.^{2} and 8 stitches/in.^{2} but it can be chosen from the range 0–16 stitches/in.^{2}). Of course, like in any stitched product, TRANSONITE® sandwiches face a compromise between improving the through-thickness properties and possible reduction of in-plane properties due to some damage imparted on the in-plane fibers by stitching. Quantifying this issue was not among objectives of this paper. Note that if stitching is not applied, the two assemblies

[1] Further details of this foam construction, properties and applications can be found on website http://www.dowcorefoams.com.

[2] See information about this product on website http://www.martinmarietta.com/Products/transonite.asp.

Please cite this article in press as: Tekalur SA et al., Shock loading response of sandwich panels with 3-D woven E-glass composite skins ..., Compos Sci Technol (2008), doi:10.1016/j.compscitech.2008.03.017

Table 1
Construction of the sandwich composite specimens used in this study

Specimen name	Front skin	Back skin	Average front skin thickness	Average back skin thickness	Stitching density per in.^{2}
Sandwich 1 ($R = 0$)	2 Layers of A + 3 layers of B	2 Layers of B + 2 layers of A	8.38 mm	6.35 mm	0
Sandwich 2 ($R = 4$)	2 Layers of A + 3 layers of B	2 Layers of B + 2 layers of A	8.18 mm	6.29 mm	4
Sandwich 3 ($R = 8$)	2 Layers of A + 3 layers of B	2 Layers of B + 2 layers of A	10.72 mm	8.11 mm	8

Note: A – 0.81 kg/m^2 E-glass plain weave; B – 3.25 kg/m^2 E-glass 3WEAVE^{TM}.

of skin fabric layers and foam core between them is directly used in pultrusion.

The difference between standard TRANSONITE® sandwich and the specialty product used in this study is, that 12 layers of 0.81 kg/m^2 (24 oz/yd^2) areal density E-glass plain weave in the front skin and eight layers of same in the back skin were replaced by three and two layers of 3.25 kg/m^2 (96 oz/yd^2) areal density 3WEAVE® fabric. This reduced labor cost and provided some other benefits to the product. Along with varying skin thickness and stitch density, sandwich panel can also be manufactured to specific dimensions: width between 15 and 260 cm, skin thickness between 2.5 and 12.7 mm, sandwich thickness between 12.7 and 101 mm. The technology is capable of providing either a consistent insertion density over a given area or localized reinforcements if needed.

To begin the pultrusion process, varying layers of fabrics are pulled together to produce the desired thicknesses of top and bottom skin preforms. Then foam layer is inserted between the top and bottom layers of the fabric forming a sandwich and subsequently the stitching is performed. Once the resin is infused, the sandwich is drawn through a heated die forming a cured composite sandwich. Finally, the panel is cut to the appropriate length. The pultrusion process is continuous. The range of mechanical characteristics observed in the sandwich composite is currently under independent evaluation. An extensive testing program is currently being conducted at North Carolina State University and at the Center for Composite Materials, University of Delaware. Independent compressive tests performed by 3TEX on a series of sandwich samples (having in-plane dimensions 6.5 × 6.5 cm and 14.5 × 14.5 cm) with 4 stitches/in.^{2} insertion density gave compressive modulus in the range 125–175 MPa and compressive strength in the range 2.2–2.6 MPa. The effective properties of these sandwiches are explained in Section 5.2.

The sandwich construction parameters are summarized in Table 1. Sandwich 1 was not stitched through the thickness ($R = 0$); the skin preforms and foam core were simply attached to each other and pultruded. In the cases of sandwich 2 and sandwich 3, the E-glass fabric preforms used for the skins were stitched together with the core in through-thickness direction and then pultruded. Core thickness in sandwich 1 and sandwich 2 was close to 50 mm, while in sandwich 3 it was considerably smaller. Due to specifics of pultrusion process, the smaller core thickness was compensated by formation of additional resin-rich layers on each side between the fabric layer closest to the core and the core surface. The skin thickness data in Table 1 for sample 3 include thickness of such additional resin-rich layer, which explains significant discrepancy between the skin thickness characteristics for sandwich 1 and sandwich 2 on one side, and for sandwich 3 on the other. Thickness of all three sandwiches was ~65.5 mm.

3. Experimental method

3.1. Loading apparatus – shock tube

Fig. 2 depicts the shock tube apparatus used in this study to obtain the controlled dynamic loading. Complete description of the shock tube and its calibration can be found in [14]. In principle, the shock tube consists of a long rigid cylinder, divided into a high-pressure driver section and a low pressure driven section, which are separated by a diaphragm. By pressurizing the high-pressure section, a pressure difference across the diaphragm is created. When this difference reaches a critical value, the diaphragm ruptures. The following rapid release of gas creates a shock wave, which travels down the tube to impart dynamic loading on the specimen. The specimen is held in fixture that ensures proper specified boundary conditions.

The shock tube utilized in the present study has an overall length of 8 m, consisting of a driver, driven and muzzle sections. The diameter of the driver and driven section is 0.15 m. The final muzzle diameter is 0.07 m. A pressure sensor (PCBA23) mounted at the end of the muzzle section measures the incident shock pressure and the reflected shock pressure during the experiment. All the sandwich composite specimens were subjected to the same level of pressure in the experiment and the pressure profile obtained at the sensor location is shown in Fig. 3. The velocity of the shock wave was measured using trigger circuits and has been determined as ~1100 m/s (Mach 3.3) in these experiments.

3.2. Boundary conditions

Rectangular flat sandwich specimens were utilized for the present experimental study. They were initially held under simply supported boundary conditions, as shown in Fig. 4. The specimen was allowed to rest vertically on two knife edges that ran along the entire width of the specimen and the size of the specimen was 30 cm × 10.2 cm. The span between supports was 15.2 cm. The dynamic loading was applied over a central circular area 7.6 cm in diameter.

Fig. 2. The URI shock tube facility.

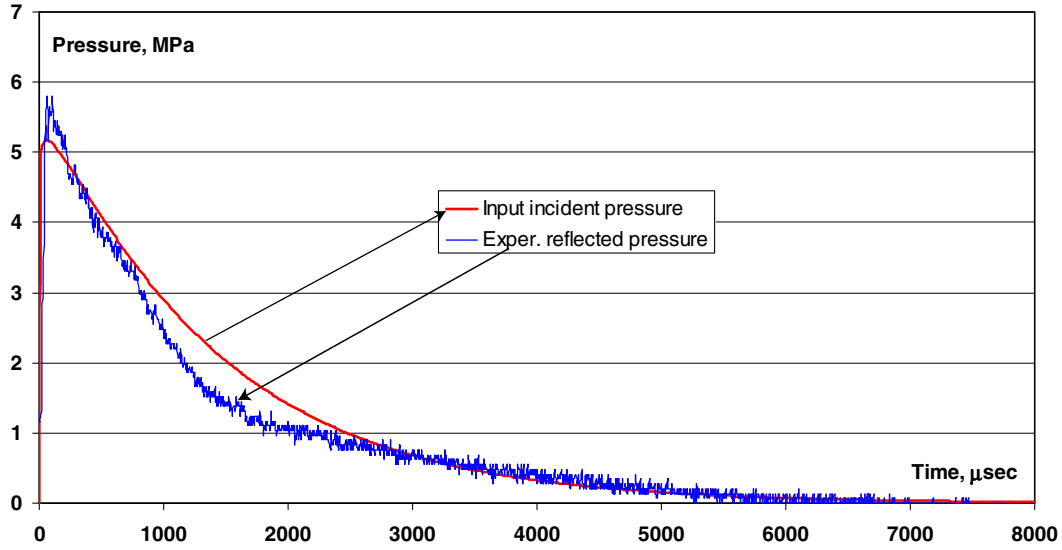

Fig. 3. Typical measured incident dynamic pressure profile (experimental). The profile used in the modeling is shown in red (theoretical). (For interpretation of the references to colour in this figure legend, the reader is referred to the web version of this article.)

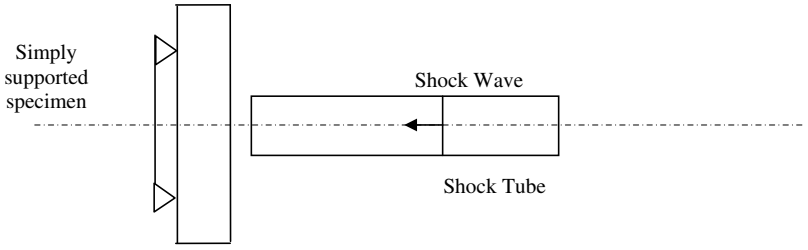

Fig. 4. Schematic of the simply supported sandwich composite specimen.

4. Experimental results

4.1. Real time transient deformation and failure observations

The dynamic transient behavior of sandwich specimens under applied shock loading was recorded using a high-speed digital camera and thoroughly analyzed. The inter-frame time utilized in the current study was 100 μs with exposure times in the order of 0.5–1.0 μs. The analysis of the high-speed images is detailed in this section for each of the test specimens, namely sandwich 1, sandwich 2 and sandwich 3.

The real time observation of shock loading of sandwich 1 is shown in Fig. 5. In this unstitched sandwich specimen, there is a soft foam core between the skins. Owing to that, the back skin remains nearly undeformed even at 500 μs time instant, while the front skin has been already deeply indented into the core, and the core itself has been severely damaged. In fact, in this case the front and back skins deform almost independently, and the high dynamic pressure applied to the front skin is substantially weakened when it reaches the back skin. The measurements showed that at 500 μs time instant, central deflection magnitude was about 5.5 times higher for the front skin than for the back one. Also seen in Fig. 5 is the initial separation at one of the sandwich edges between the front skin and the core at 200 μs time instant, which indicates high stress concentration at the front skin-core interface along the sample edges. The indentation failure of the front skin is observed from 200 μs time. The onset of core failure is observed at 400 μs time, and complete collapse of the core is seen at 500 μs time instant. The conclusion is that for sandwich 1, all important deformation, damage initiation and total failure events had occurred within 0.5 ms time from the shock wave arrival.

The first principal failure mechanism evident in Fig. 5 is progressive damage of the core, which starts with some dispersed damage near the front skin and simultaneous formation of a large inclined crack in the central region of the core. These two damage zones gradually extend and coalesce at approximately 400 μs time instant which is followed by the formation of a much larger damage zone at 500 μs time instant and rapid crush of the core after that time instant. Possibly, around the same time the front skin suffers significant failure (and hence loses most of support from the core), although it is difficult to see it in Fig. 5. Likely, the back skin fails soon after that, and the whole sandwich is crushed. The conclusion is that sandwich 1 does not provide sufficient transient load transfer from the front skin to the back skin and, as a result, it cannot withstand the applied dynamic pressure which has peak value ~5.24 MPa reached at $\sim t = 60$ μs (the pressure history is of the type shown in Fig. 3).

Fig. 6 details corresponding real time observations for sandwich 2. In this case it is seen that the dynamic pressure is much better transferred from the front to the back of the sandwich, and we see well synchronized local bending of both skins. The core is gradually damaged as the skin bending progresses. As the measurements showed, the difference between central deflection values of the front and back skins is relatively small. Also, no separation between the front skin and the core is seen in these high-speed camera frames, thus the aforementioned high stress concentration for sandwich 1 at the skin-core interface has been reduced by core stitching. Failure mode of this stitched sandwich can be defined as

Please cite this article in press as: Tekalur SA et al., Shock loading response of sandwich panels with 3-D woven E-glass composite skins ..., Compos Sci Technol (2008), doi:10.1016/j.compscitech.2008.03.017

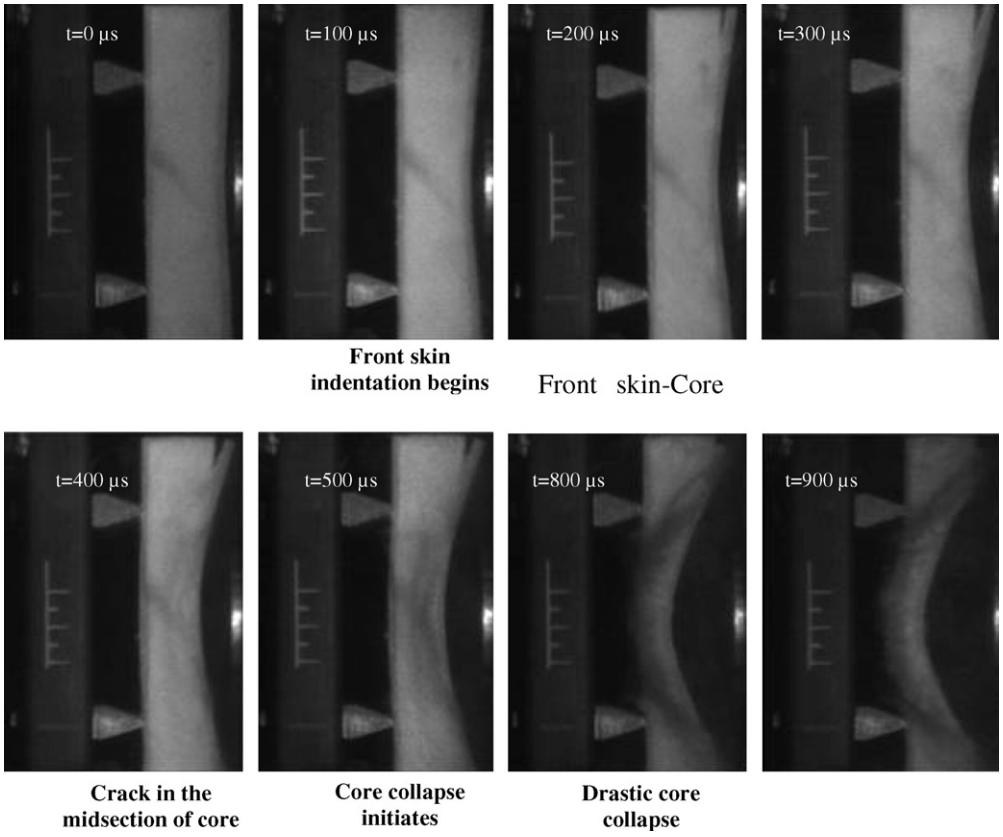

Fig. 5. Real-time observation of sandwich 1 using high-speed camera.

a combination of core shear and face failure types. The first two frames (up to 100 μs time instant) do not reveal any macroscopic damage to the sandwich. At 200 μs time instant initial cracks are seen in the core; they start in the mid-section of the core in the direction preferably parallel to the loading plane. The transition of "hinge point" takes place between time instants 300 and 800 μs. Further, at time instant 900 μs, the cracks in the core become more pronounced and the "hinging" of the whole sandwich (including the span and overhang) along a center line can be observed.

Fig. 7 illustrates the deformation process of sandwich 3. This appears to be very similar to the one seen in Fig. 6. Though on a closer observation, two significant differences in the real time deformation can be detailed. The first difference is that the deflection values at 500 μs time instant are by 30% smaller at the center of the specimen in this case than for sandwich 2. This can be attributed to the two factors: (a) more dense core stitching and (b) resin layers compensating for reduced thickness of the foam core material in sandwich 3. Both factors provide additional stiffening to the sandwich. The second difference is in the deformation and failure progression. It is observed that at 100 μs time instant there are no visible cracks in the core and the overhangs of the simply supported sandwich are straight, whereas the span portion is hinged about the support lines. The hinge point moves from the support line to the center of the sandwich as the time progresses, which is seen between time instants 200 and 400 μs. Further on, at 700 μs time instant the transition is completed and the whole sandwich is hinged about the center.

So, in contrast to the results shown in Fig. 5 for sandwich 1, the real time deformation sequences shown in Fig. 6 for sandwich 2 and in Fig. 7 for sandwich 3 indicate that the reinforced core damage does not include any visible macro-cracks, although one can see certain micro-damage accumulation and propagation from frame to frame. Further, it is hard to detect any skin damage and failure peculiarities in Figs. 6 and 7. In order to get a better understanding of this aspect, additional post-mortem evaluation of the tested sandwich panels has been performed as discussed in the next section.

The principal conclusion made from these experimental results is, that through-thickness stitching of the sandwich before resin infusion makes a remarkable positive effect on the transient deformation, damage initiation and progression processes in the studied sandwich materials. The major failure modes observed in this study under the transient loading conditions are sketched in Fig. 8. These failure modes can be broadly classified as (a) front skin indentation (b) core shear failure and (c) skin failure. No doubt that a more scrupulous investigation would reveal that each of these failure modes has certain "branches" that are more or less pronounced at different time intervals for distinctive sandwich constructions. For example, in the case (b) cracks both perpendicular and parallel to the loading direction were observed. Hence, unlike in respective static loading case, where given load type usually corresponds to a well-defined, dominating single failure mode, in the case of highly transient dynamic loading (as in this study) the initiation and development of more than one different failure modes can be observed simultaneously.

4.2. Macroscopic post-mortem evaluation

Results of post-mortem evaluation of the shock wave tested sandwich composite panels are shown in Figs. 9–11. In sandwich 1 case, the core did disintegrate completely when tested and was lost beyond retrieval. The front skin (which is in the top in Fig. 9) shows severely fractured fibers in the central region (where dynamic pressure was applied); it was also frac-

Please cite this article in press as: Tekalur SA et al., Shock loading response of sandwich panels with 3-D woven E-glass composite skins ..., Compos Sci Technol (2008), doi:10.1016/j.compscitech.2008.03.017

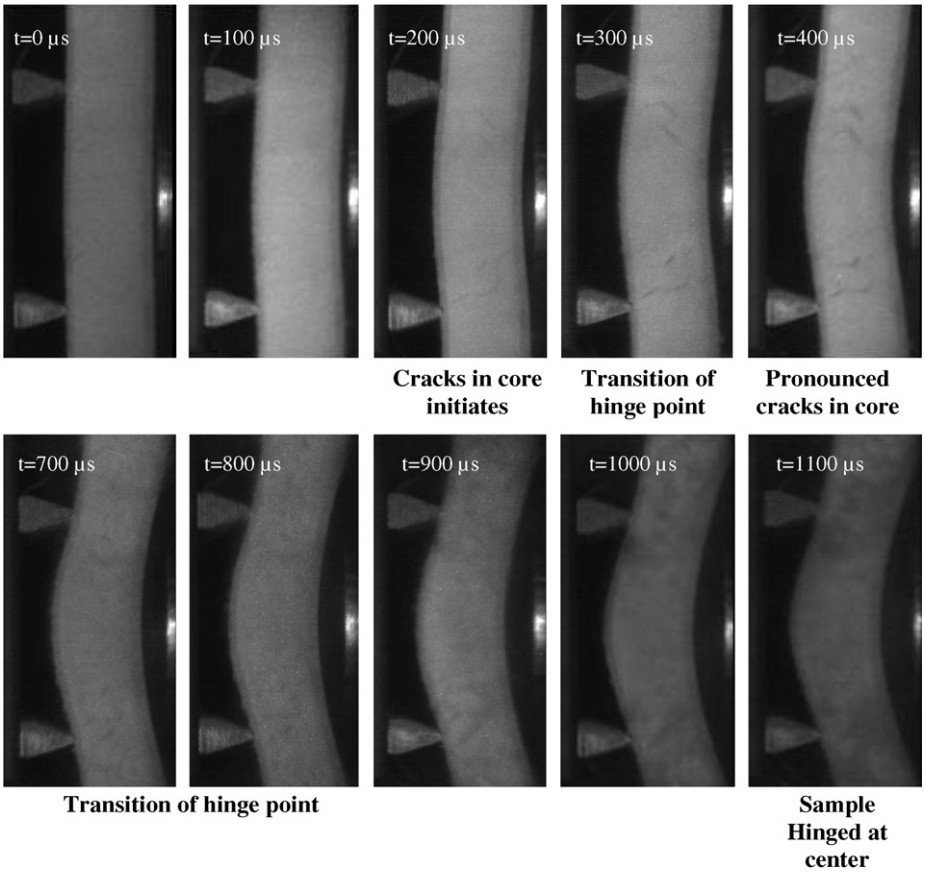

Fig. 6. Real-time observation of sandwich 2 using high-speed camera.

tured into two layers there. The back skin did completely delaminate along the interface between two 3-D woven composite layers and separated into two pieces having thicknesses 2.92 mm and 3.86 mm.

Contrary to the above, Fig. 10 shows only localized delaminations in the skins accompanied by the foam damage in the core. The damage in this case is confined to the mid-section of the front skin; minimal visual damage is observed in the back skin. The observed residual deformation of this sandwich sample is relatively small. Separation of the core chunks from the vertical stitch composite bars are seen in this sample. Buckling of the stitch bars themselves was observed under close-up visual examination. The location of such local buckling was identified by bright white shear-like spots on the side view of the sandwiches. Such bright white spots were detected closer to either one of the skins rather than in the mid-region of the core. It was also observed that micro-delaminations appeared within the skin of this sandwich specimen.

Further on, Fig. 11 shows very minimal damage in the skins and core and practically no global permanent deformation of sandwich 3. Both front and back skins show no signs of fiber breakage or other failure types. Only small cracks parallel to the stitches were found in the core, and small micro-delamination cracks are present in the skins. Overall, it can be concluded that this sandwich had survived the shock loading significantly better than sandwich 2 and did not lose its overall integrity. As pointed our before, this improvement can be attributed to the higher stitching density and to the the marginal increase in the thickness of the skin (which replaces the corresponding foam material in the core).

4.3. A summary of deflection history observations

The high-speed images presented in Section 4.1 were further analyzed in order to measure the dynamic deflections of the rear face and the front face of the shock loaded sandwiches 1, 2 and 3. The quantitative differences in the deflection histories are clearly seen in Fig. 12.

In sandwich 1 having unstitched core, the strike face deflections were 3–4 times higher than the rear face deflections during the first 500 μs time interval, and the difference kept further increasing with time. Sandwich 1 also suffered the largest front face deflection (curve 1F in Fig. 12), which reached approximately five times of its front skin thickness. At the same time, the rear face deflection (curve 1R in Fig. 12) was less than one thickness of the rear skin. The difference between the front and rear skin dynamic deflections for sandwich 1 is much higher than that observed for sandwiches 2 and 3.

Further on, it is seen in Fig. 12 that dynamic deflections of both skins in sandwich 2 (curves 2F and 2R) grow linearly with time, and they do not show any trend to reach maximum up to 1200 μs time instant. Contrary to that, dynamic deflections of both skins in sandwich 3 (curves 3F and 3R) reach maximum at approximately 800 μs time instant. The magnitude of this maximum is about 7 mm, which is below one thickness of the front skin and also is three times lower than the dynamic deflection of sandwich 2 at 1200 μs time instant. Of course, further reduction of the maximum dynamic deflection is possible by increasing stitching density. It should be emphasized again that, according to results discussed before, the increase of stitching density also resulted in significant reduction of damage imparted to the tested sandwich specimens.

Please cite this article in press as: Tekalur SA et al., Shock loading response of sandwich panels with 3-D woven E-glass composite skins ..., Compos Sci Technol (2008), doi:10.1016/j.compscitech.2008.03.017

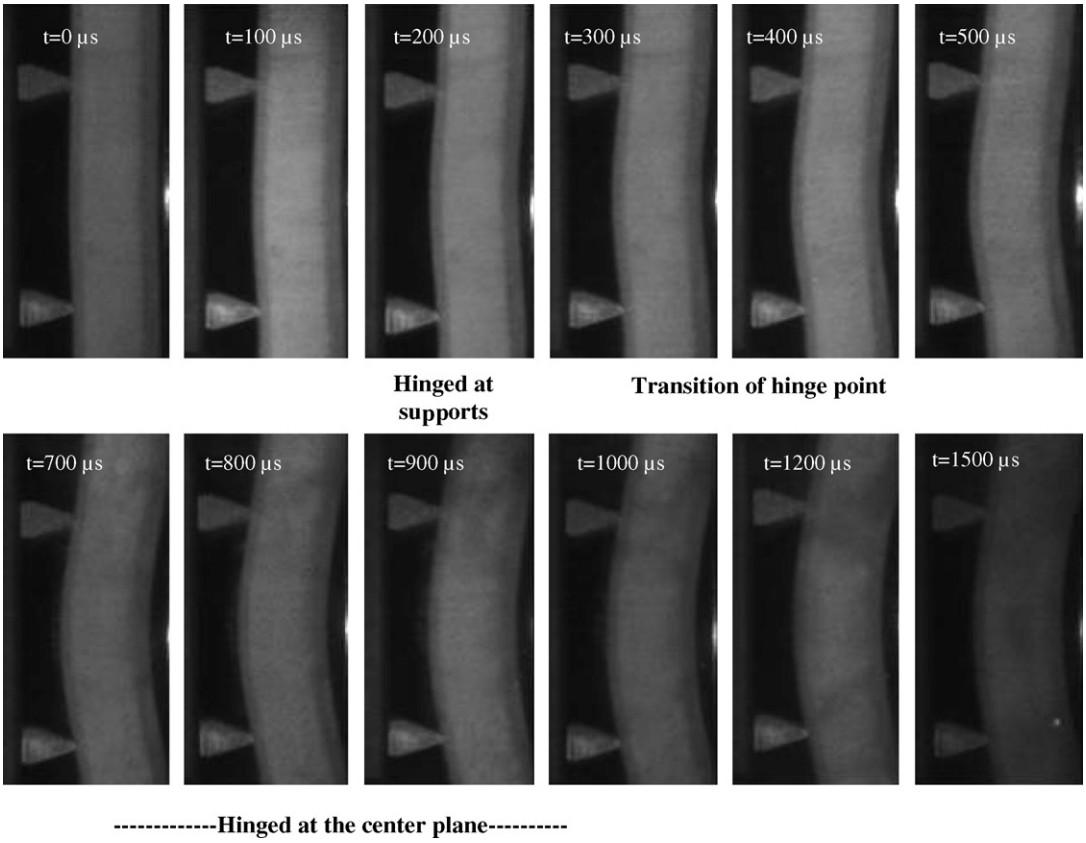

Fig. 7. Real-time observation of sandwich 3 using high-speed camera.

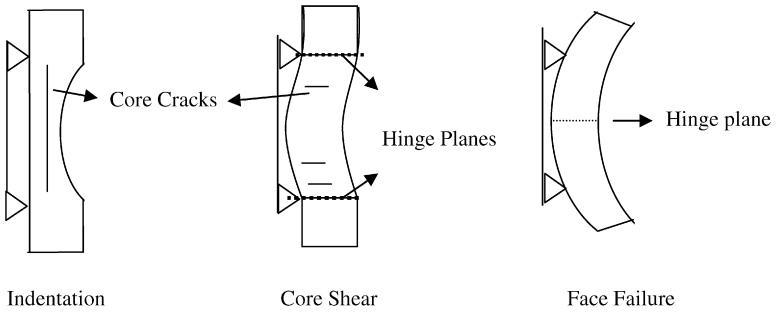

Fig. 8. Principal failure modes observed in sandwich samples under shock loading.

5. Computational modeling of shock wave loaded sandwich panels

In continuation of this research work, the shock wave loading of sandwich 1, sandwich 2 and sandwich 3 test specimens was simulated using 3-D MOSAIC analysis approach briefly described in Section 1 (see further details in [15,16]) and 3TEX's in-house computer code. The obtained results allowed us to directly compare experimental data for dynamic deflection included in Fig. 12 and the respective theoretical predictions. The 3-D dynamic boundary value problem formulation and selected results of the performed theoretical study are presented in this section.

5.1. 3-D dynamic boundary value problem formulation

Test specimens used in the experimental study had rectangular shape, and their measured dimensions in x, y and z directions were as follows:

$$2a = 0.3048\ \text{m}, \quad 2b = 0.1016\ \text{m}, \quad c = 65.53\ \text{mm}, \tag{1}$$

where $2a$, $2b$ and c are full length, width and thickness of the sandwich, respectively; the values listed in (1) we used in the analysis of sandwich 1, 2 and 3 specimens.

Further, notations c_1, c_2 and c_3 are used in the three layer model of sandwiches 1 and 2 (see Fig. 13a) for thicknesses of the back skin, core and front skin, respectively. Their values were measured at numerous locations and the average magnitudes were determined as follows for sandwich 1:

$$c_1 = 6.35\ \text{mm}, \quad c_2 = 50.80\ \text{mm}, \quad c_3 = 8.38\ \text{mm} \tag{2}$$

and for sandwich 2

$$c_1 = 6.29\ \text{mm}, \quad c_2 = 51.06\ \text{mm}, \quad c_3 = 8.18\ \text{mm} \tag{3}$$

A five layer model shown in Fig. 13b was used for sandwich 3. Additional two layers of pure resin between each skin and the core were introduced here in order to correctly account for the manufacturing peculiarity of this sandwich (those were described in Section 2.3). Now, we have the following five thickness characteristics:

Please cite this article in press as: Tekalur SA et al., Shock loading response of sandwich panels with 3-D woven E-glass composite skins ..., Compos Sci Technol (2008), doi:10.1016/j.compscitech.2008.03.017

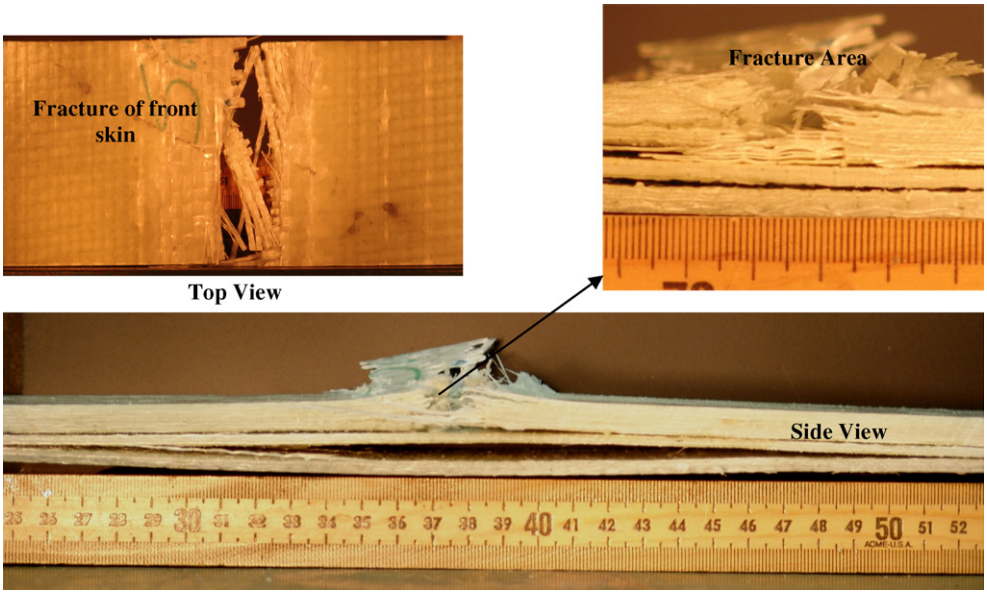

Fig. 9. Post-mortem evaluation of sandwich 1.

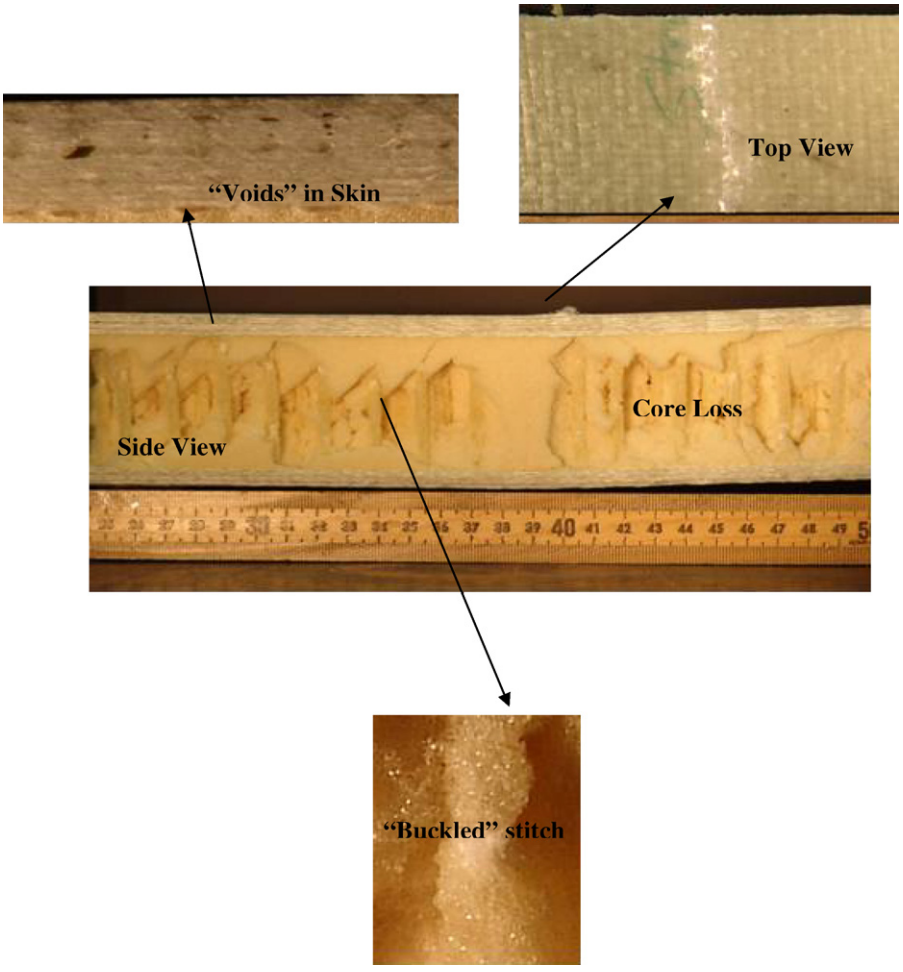

Fig. 10. Post-mortem evaluation of sandwich 2.

$$c_1 = 6.35\ \text{mm}, \quad c_2 = 1.76\ \text{mm}, \quad c_3 = 46.7\ \text{mm}, \quad c_4 = 2.34\ \text{mm}, \quad c_5 = 8.38\ \text{mm} \tag{4}$$

The following boundary conditions were imposed. The experimental specimens were placed on rigid supports which are oriented in

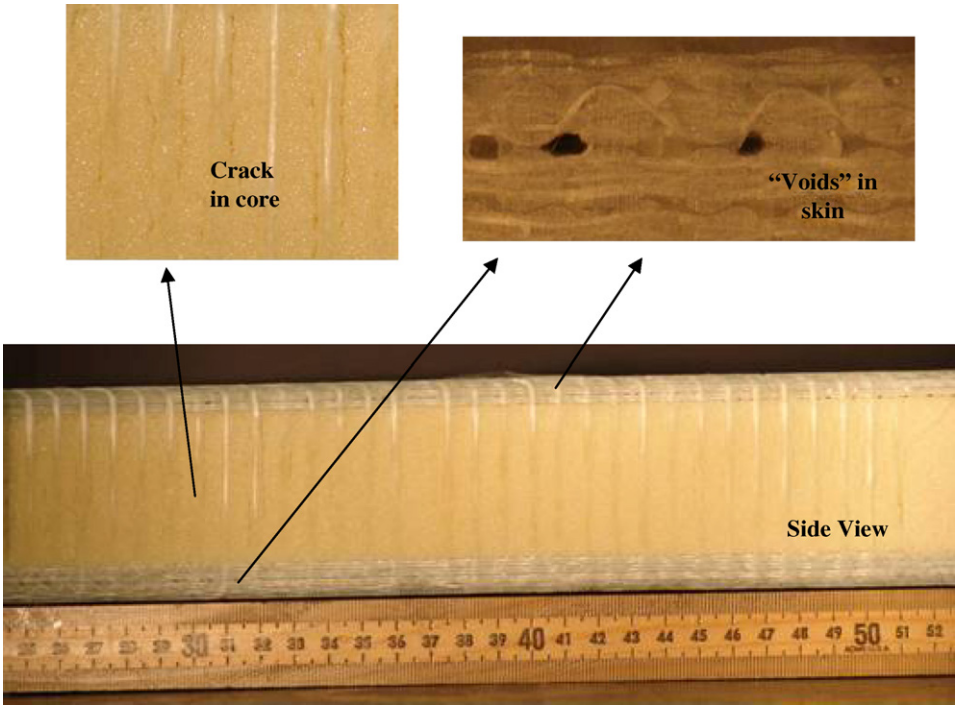

Fig. 11. Post-mortem evaluation of sandwich 3.

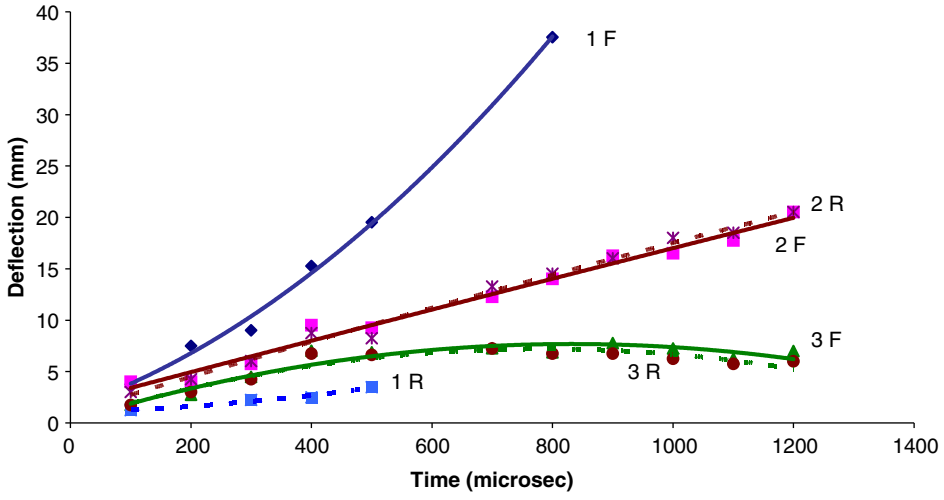

Fig. 12. Time–deflection histories of the front face (1F, 2F, 3F) and rear face (1R, 2R, 3R) of sandwiches 1, 2 and 3.

y-direction. The specimen length outside each support is $a_1 = 0.076$ m. We assume here that the support width is $a_2 = 0.4$ mm. Although this parameter was not exactly determined and may slightly influence the analysis results for central deflection, we believe that the value taken was sufficiently small to not make a considerable effect. The distance from support to the center of the specimen is $a_3 = 0.076$ m. Another geometric parameter is associated with the loading area, which is assumed to be a square with side length $2a_0 = 0.06751$ m; this length was calculated as to equalize the square area to the area of a circle with diameter $d = 0.0762$ m, which is the actual loading area in the shock tube experiments.

Due to the symmetry of the boundary value problem under consideration, the analysis can be reduced to 1/4 of the panel, with the following symmetry conditions added:

$$u_x = 0 \text{ at } x = a \quad \text{for all } z \tag{5}$$

$$u_y = 0 \text{ at } y = a \quad \text{for all } z \tag{6}$$

The following boundary condition is applied within rigid support area:

$$u_z = 0 \text{ at } a_1 \leqslant x \leqslant a_1 + a_2 \text{ for all } y \tag{7}$$

Further, it is assumed that central region of the top surface of the plate is loaded by dynamic pressure distributed according to a half-sine law within square region $2a_0 \times 2a_0$ ($2a_0$ has been quantified above). Hence, the loaded region of 1/4 of the panel is defined as

$$a - a_0 \leqslant x \leqslant a; \quad b - a_0 \leqslant y \leqslant b \text{ at } z = c \tag{8}$$

The time variation of blast pressure acting on the specimen is taken in the form

Please cite this article in press as: Tekalur SA et al., Shock loading response of sandwich panels with 3-D woven E-glass composite skins ..., Compos Sci Technol (2008), doi:10.1016/j.compscitech.2008.03.017

$$P(t) = P_0 \times t^n \times e^{-B \cdot t} \quad (9)$$

which well corresponds to the experimental shock wave incident pressure history shown in Fig. 3. Here, t is measured in μs, P_0 and $P(t)$ in MPa. The following numerical parameters were determined for (9) from the smooth approximation of experimental reflected pressure recorded in experiments:

$$P_0 = 5.167 \text{ MPa}, \quad n = 0.045, \quad B = 0.00075 \ \mu s^{-1} \quad (10)$$

These values provide the peak pressure magnitude $P(t_0)$ = 5.167 MPa which is reached at t_0 = 60 μs time instant.

In the conducted shock tube experiments, surface distribution of the incident pressure should be close to uniform. However, due to some computational reasons, in the analysis the surface load distribution was taken in the form of half-sine wave along both coordinates x and y. Accordingly, the P_0 magnitude in (10) has to been increased by factor $(\pi/2)^2$ in order to keep equivalency between integral pressure values acting on the panel in both cases. So, in all analysis runs the value P_0 = 12.75 MPa at the center of the panel has been adopted. The other parameters in (10) remained unchanged. A comparison of the measured experimental pressure and the input pressure used in the computational model using Eqs. (9,10) is also shown in Fig. 3.

5.2. Material properties

The material property inputs for the performed analysis require effective elastic properties of the front and back composite skins (which were fully homogenized) and effective elastic properties of the cores (which were also fully homogenized). It has to be noted that such homogenization is not essential for the utilization of 3-D MOSAIC analysis approach and computer code. Particularly, each individual layer of 2-D woven and 3-D woven fabric composites (identified in Table 1) within front and back skins can be homogenized individually or, if necessary, modeled at its unit cell level, as demonstrated on some static analysis problems in [18,24]. Such a model refinement for the skin materials would be purposeful when analyzing damage and failure problems, but those are not considered here. Also importantly, the elastic properties of all composite layers in the skins are very close, which gives another good reason for the full skin homogenization. Some other analysis applications can be found in [19,20], where thick layered and sandwich panels were composed of polymeric composites, ceramics, balsa wood and concrete materials in different combinations. Each layer in those structures was individually homogenized, and the layered panels characterized by huge step-wise variations of through-thickness properties were solved under blast wave induced transient pressure.

The above said also applies to the foam core homogenization. 3-D MOSAIC analysis approach allows one to solve transient deformation problems, where a stitched foam core is treated as two-phase composite with foam as the matrix and through-thickness reinforcement as uniformly spaced, parallel unidirectional E-glass composite bars. Of course, this level of core modeling would be very useful when analyzing damage and progressive failure processes in the core.

Considering known elastic properties of E-glass fiber, defined reinforcement architecture of the fabrics in the skins and known elastic properties of Derakane 8084 epoxy–vinyl ester resin, the following effective elastic properties of the skins were obtained by stiffness averaging method:

$$E_x = 25.1 \text{ GPa}, \quad E_y = 25.6 \text{ GPa}, \quad E_z = 12.5 \text{ GPa} \quad (11)$$

$$G_{xy} = G_{xz} = 3.5 \text{ GPa}, \quad G_{yz} = 3.3 \text{ GPa} \quad (12)$$

$$\nu_{xy} = 0.13, \quad \nu_{xz} = 0.34, \quad \nu_{yz} = 0.33 \quad (13)$$

These values are in a close agreement with available effective elastic properties of 3-D woven and 2-D woven E-glass composites with ~50% fiber volume fraction. In addition, the following density value was used in the analysis: ρ = 1850 kg/m^3.

The principal elastic properties of the foam core were taken as suggested in the manufacturer's specifications:

$$E_c = 5.17 \text{ MPa}, \quad G_r = 1.79 \text{ MPa}, \quad \nu = 0.44, \quad \rho = 32.0 \text{ kg/m}^3 \quad (14)$$

Here E_c is compressive modulus, G_r is shear modulus parallel to rise, ν is Poisson's ratio, and ρ is foam density. Along with this pristine form, two hypothetical "damaged foam" materials (with E_c and G_r arbitrarily reduced by factor of 10 and by factor of 100) have been considered in the analysis. The respective elastic properties are as follows:

$$E_c = 0.517 \text{ MPa}, \quad G_r = 0.179 \text{ MPa}, \quad \nu = 0.44, \quad \rho = 32.0 \text{ kg/m}^3 \quad (15)$$

$$E_c = 0.0517 \text{ MPa}, \quad G_r = 0.0179 \text{ MPa}, \quad \nu = 0.44, \quad \rho = 32.0 \text{ kg/m}^3 \quad (16)$$

In the property variants (14)–(16) the foam was considered as isotropic material.

Effective elastic properties of the foam cores reinforced with parallel stitches of E-glass roving were computed with the use of stiffness averaging method by assuming that a stitched core is a unidirectional composite, where foam (having properties (14)) serves as the matrix in which straight and aligned in through-thickness direction E-glass fibers are embedded. Specifically, 0.37% and 0.74% volume fractions of fibers were evaluated for the cases of 4 and 8 stitch/in.^{2} insertion densities, respectively. The resulting effective elastic properties are (axes x and y are in-plane, axis z goes through the thickness):

$$E_x = E_y = 6.15 \text{ MPa}, \quad E_z = 135 \text{ MPa}, \quad G_{xy} = G_{xz} = G_{yz} = 1.86 \text{ MPa}, \quad \nu_{xy} = 0.65, \quad \nu_{zx} = \nu_{zy} = 0.4, \quad \rho = 38.8 \text{ kg/m}^3 \quad (17)$$

for the case of sandwich 2 and

$$E_x = E_y = 6.20 \text{ MPa}, \quad E_z = 265 \text{ MPa}, \quad G_{xy} = G_{xz} = G_{yz} = 1.87 \text{ MPa}, \quad \nu_{xy} = 0.66, \quad \nu_{zx} = \nu_{zy} = 0.4, \quad \rho = 45.5 \text{ kg/m}^3 \quad (18)$$

for the case of sandwich 3. Also, in addition to (17), numerical simulations were performed for the following properties of sandwich 2 (E_z, G_{xz} and G_{yz} were arbitrarily reduced by factor of 5):

$$E_x = E_y = 6.15 \text{ MPa}, \quad E_z = 27 \text{ MPa}, \quad G_{xy} = 1.86 \text{ MPa}, \quad G_{xz} = G_{yz} = 0.372 \text{ MPa}, \quad \nu_{xy} = 0.65, \quad \nu_{zx} = \nu_{zy} = 0.4, \quad \rho = 38.8 \text{ kg/m}^3 \quad (19)$$

Also, the isotropic properties of Derakane 8084 resin which characterize layers 2 and 3 of the five layer model used in sandwich 3 analysis, were taken as follows:

$$E = 2.9 \text{ GPa}, \ \nu = 0.35, \ G = 1.1 \text{ GPa}, \ \rho = 1.14 \text{ g/cm}^3 \quad (20)$$

5.3. Some computational aspects

The analyzed 1/4 of the experimentally studied sandwich panel models are shown in Fig. 13 together with an illustrative computational mesh. A three layer model (a) was used for sandwiches 1 and 2, while a five layer model (b) was used for sandwich 3.

In this specific case, the body is non-uniformly discretized into three parts in x direction, two parts in y direction, while no discretization is used for the skins and core in z direction. 3-D MOSAIC analysis allows one to increase accuracy of results in two

Please cite this article in press as: Tekalur SA et al., Shock loading response of sandwich panels with 3-D woven E-glass composite skins ..., Compos Sci Technol (2008), doi:10.1016/j.compscitech.2008.03.017

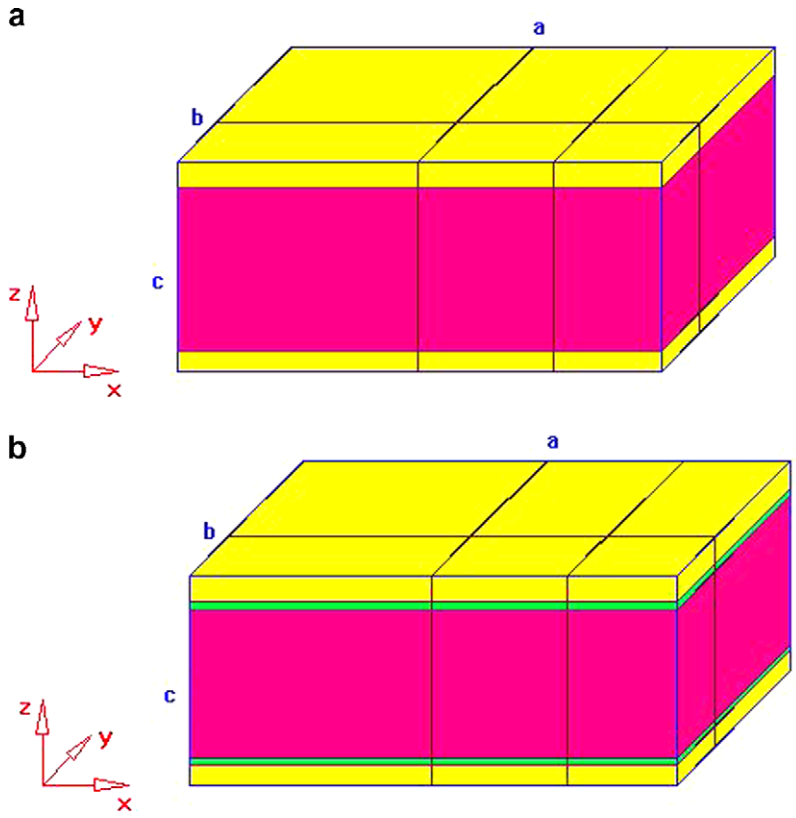

Fig. 13. One quarter of sandwich panel models: three layer model (a) used for sandwich 1 and sandwich 2, and five-layer model (b) used for sandwich 3.

independent ways – by refining discretization mesh and by increasing degree of the basis functions (Bernstein approximation polynomials), see [15,16]. Either way ultimately results in the same converged numerical solution. However, the path to that converged solution may be more or less lengthy, depending on specific problem. Using same amount of degrees of freedom with a higher polynomial degree but lower number of discretization intervals typically results in a more accurate solution than if using a lower polynomial degree with finer discretization. Numerical results presented in this section were verified for convergence using both ways. Specifically, all displacement, strain and stress characteristics were computed with the use of 2nd and 3rd degree basis functions for several uniform and non-uniform discretization meshes. The results shown here correspond to solutions which looked converged.

Another important notice is that the difficulty of accurately predicting different displacement, strain and stress characteristics varies enormously. Typically, the easiest ones are displacements, more difficult are in-plane strains and stresses, next are transverse shear strains and stresses, transverse normal strain, and the ultimate challenge is to accurately predict transverse normal stress. At the same time, when analyzing some structure loaded by dynamic force within a region on its face surface, the computed transverse normal stress history $\sigma_z(t)$ has to be, ideally, identical to the applied pressure history (in our case, the latter is one defined by Eqs. (9) and (10)) at any point of that loaded area. However, in any displacement-assumed structural analysis approach, the surface force boundary conditions are not imposed directly, and those two functions will never be identical. This is why demonstrating convergence of the computed stress component $\sigma_z(t)$ to the applied pressure history $P(t)$ is the best way of validating sufficiently accuracy of the obtained numerical solution. More detailed discussion and illustrative examples on this matter can be found in [20]. Without dwelling into specific illustrations, we state here that such a convergence study has been performed for numerical examples presented in the next section.

5.4. Comparison of theoretical and experimental results

Numerical results obtained with 3-D MOSAIC dynamic analysis code are presented here for transverse displacement (deflection) history, $u_z(t)$, which was well quantified in the experimental study, see Sections 4.1 and 4.3. In all cases the deflection history was computed at the center of the panel, on the front (exposed to shock wave) and on the back (load-free) surfaces.

Numerical results for sandwich 1 specimen, together with experimental points from Fig. 12, are shown in Fig. 14 for the front face and in Fig. 15 for the back face. In Fig. 14 there are three theoretical curves corresponding to foam properties: (14) labeled 1.0, (15) labeled 0.1 and (17) labeled 0.01. While the difference between the first one and the other two is considerable, the last two practically coincide. This means that foam core with properties (14) still has some supporting effect on the front skin, while with foam properties (15) and (16) the front skin deforms practically by its own. This also indicates that any further change of the foam properties would not move these theoretical results closer to the experimental data points. Though the discrepancy is not very large, the predicted sandwich response is significantly "stiffer" than the experimental one. The reasons are not clear at this point, asking for more experimental and theoretical work in this direction.

The results presented in Fig. 15 for the back face with the same three core moduli used in analysis show much stronger effect of the 10 times moduli reduction. However, the "reduced moduli" effect is opposite to the desirable – the theoretical curves move further away from the experimental points. Yet, the whole experimental and theoretical dynamics of the back skin deflection

Please cite this article in press as: Tekalur SA et al., Shock loading response of sandwich panels with 3-D woven E-glass composite skins ..., Compos Sci Technol (2008), doi:10.1016/j.compscitech.2008.03.017

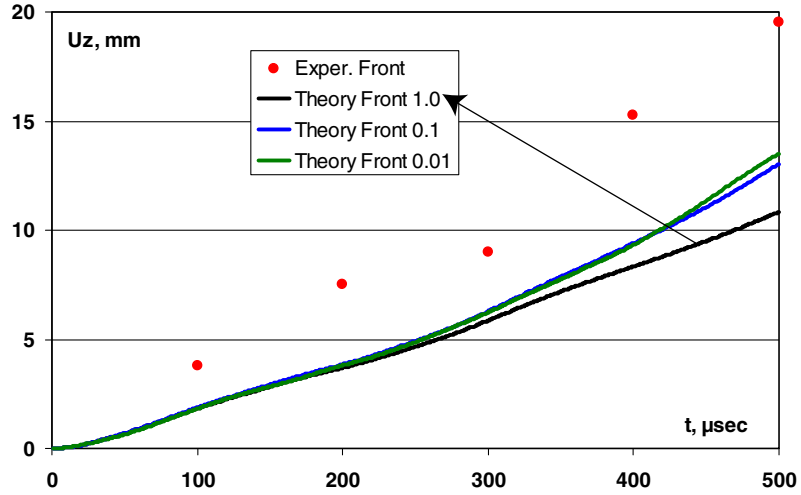

Fig. 14. Theoretical and experimental deflection vs. time results for sandwich 1 – front face.

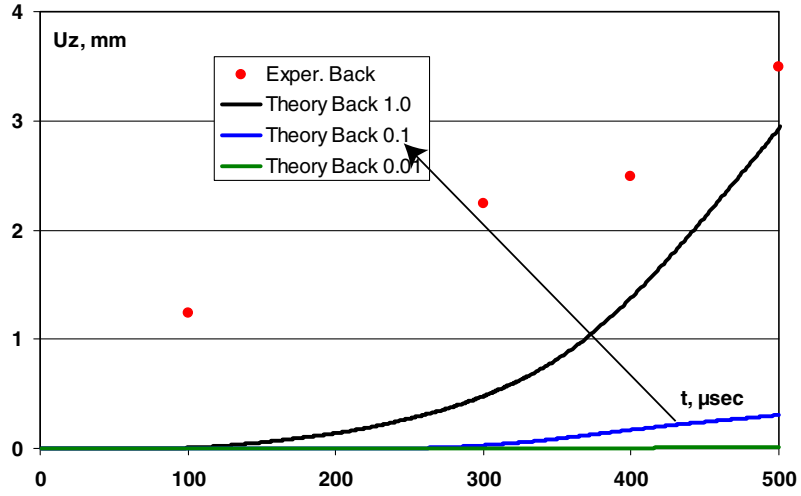

Fig. 15. Theoretical and experimental deflection vs. time results for sandwich 1 – back face.

development are quite different – the experiment shows nearly linear deflection growth, while the theory indicates a very slow growth initially, then the deflection grows with steadily increasing speed. Again, the reasons for this significant discrepancy are unclear at this point.

Figs. 16 and 17 show comparison of theoretical and experimental results for sandwich 2 specimen. In both these figures there are two theoretical curves plotted – one corresponds to the core properties (17), the other to five times reduced transverse moduli (19). In the case of front face the moduli reduction allowed to get closer to the experimental point, which indicates that core properties (17) are overestimated. This is quite surprising, because the value of transverse compressive modulus 135 MPa in (16) was taken closer to the lower end of experimental data range. Nevertheless, the comparison of theoretical and experimental data in Fig. 16 may be qualified as first success – the predicted deflection histories are similar to the trend of experimental points and provide quite close deflection values.

The comparison of theoretical and experimental results for the back skin of sandwich 2 in Fig. 17 shows larger discrepancy than the one in Fig. 16. However, the discrepancy is significantly smaller than that for unstitched sandwich 1 in Fig. 15. Also interestingly, the moduli reduction by factor of 5 moves theoretical results farther away from experimental data points. Simply, it helps in the case of front skin and hurts in the case of back one. It is hard to explain these results, or even comment on them, without additional theoretical and experimental studies.

Finally, after presenting and discussing not so close comparisons of the obtained theoretical and experimental results for sandwich 1 and sandwich 2 structures, Figs. 18 and 19 show very good agreement for both front and back faces in the case of sandwich 3. The effective elastic properties of the stitched core in this case, listed in (18), were computed with the same methodology as the effective elastic properties of sandwich 2, listed in (17), only stitch density and, therefore, the through-thickness fiber volume fraction was increased by factor of 2. See Fig. 20

6. Discussion

It is as hard to give a fully substantiated and convincing explanation to the observed discrepancy between theoretical and experimental results presented above. Of a special interest is the revealed effect that when increasing stitch density the discrepancy is reduced. This looks like a trend, not an incidental result. We can learn by now from this performed work, first of its kind, that several specific experimental and theoretical studies are required to

Please cite this article in press as: Tekalur SA et al., Shock loading response of sandwich panels with 3-D woven E-glass composite skins ..., Compos Sci Technol (2008), doi:10.1016/j.compscitech.2008.03.017

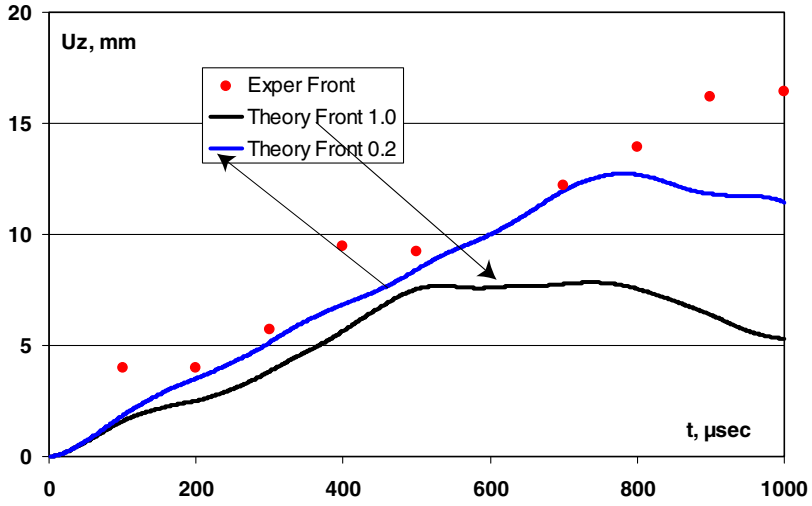

Fig. 16. Theoretical and experimental deflection vs. time results for sandwich 2 – front face.

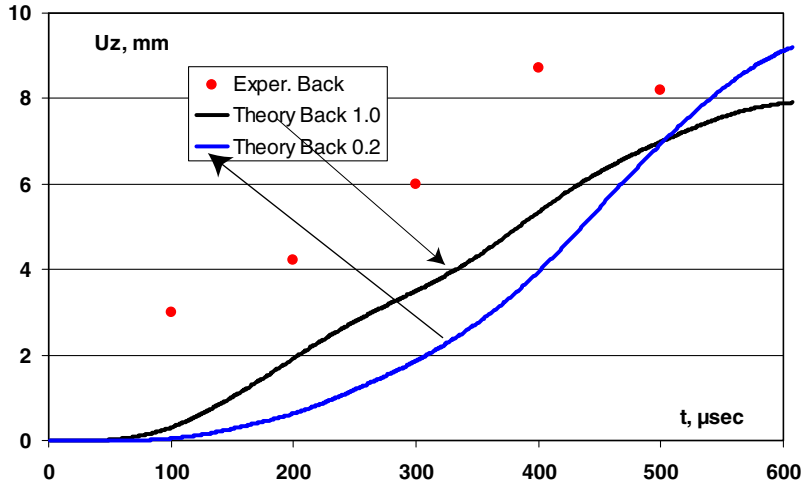

Fig. 17. Theoretical and experimental deflection vs. time results for sandwich 2 – back face.

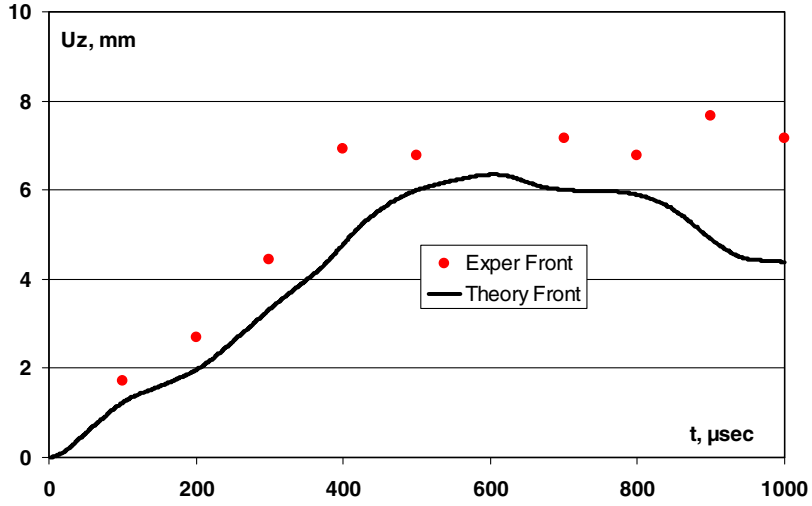

Fig. 18. Theoretical and experimental deflection vs. time results for sandwich 3 – front face.

Please cite this article in press as: Tekalur SA et al., Shock loading response of sandwich panels with 3-D woven E-glass composite skins ..., Compos Sci Technol (2008), doi:10.1016/j.compscitech.2008.03.017

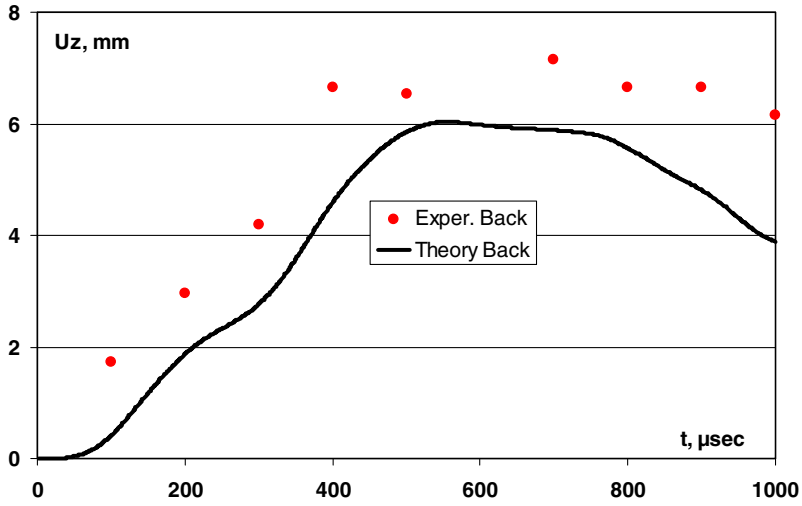

Fig. 19. Theoretical and experimental deflection vs. time results for sandwich 3 – back face.

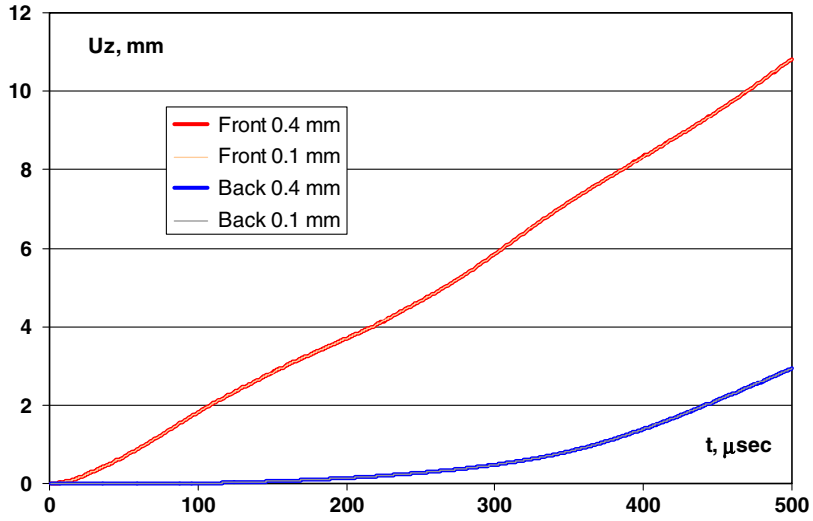

Fig. 20. Theoretical deflection vs. time curves obtained for two values of support width: 0.4 mm and 0.1 mm; the respective curves practically coincide.

identify all possible causes for the discrepancies, and then understand their qualitative effect. In this section we discuss those possible causes.

(1) Experimental and theoretical realization of simply supported plate boundary conditions. In the performed analysis we imposed the local geometric boundary condition (7), which means that transverse displacement u_z is assumed zero along its contact area with support (between x coordinates a_1 and $a_1 + a_2$). The width of the contact area, a_2, is an explicit input parameter of the code and can be changed easily. The above reported results were obtained for $a_2 = 0.4$ mm. In order to investigate the effect of this parameter on the computed deflection values, one example (sandwich 1 with core characteristics (14), black curves in Figs. 14 and 15) was additionally solved for $a_2 = 0.1$ mm value. The respective deflection–time curves are shown in Fig. 23 for both front and back surfaces. The respective two curves in each case are visually indistinguishable. In fact, the maximum difference between them is about 0.1%. Thus, this cause can be ruled out. Also note that, like in the experimental set up, in the analysis there are no geometric constraints imposed on the in-plane displacements u_x and u_y, except for the symmetry conditions (5) and (6) which prevent translation of the whole sandwich panel as a rigid body.

(2) Material properties of the cores assumed in the analysis are significantly different from those in actual sandwich structures. Though there are significant uncertainties in determining effective elastic properties of all three foam cores used in this study, it is unlikely that this factor is responsible for the observed discrepancies. First of all, elastic properties of the cores in sandwich 1 and sandwich 2 have been varied in a wide range; see Figs. 14–17. Such variations not only gave quite limited effect, but it was opposite for the front and back faces. Indeed, for the front face the reduction of core stiffness moves theoretical and experimental results farther close, while for the back face it moves them apart. At the same time, the experimental deflections are consistently above the theoretical ones for both front and back faces.

(3) There is some possibility that effective elastic properties of the composite skins (11)–(13) assumed in the analysis are much higher than those of actual composite skins in the sandwiches. Note that the former ones are based on the experimental and theoretical data for the single layer 3-D weave and 2-D weave composites, while the skins are actually made from the

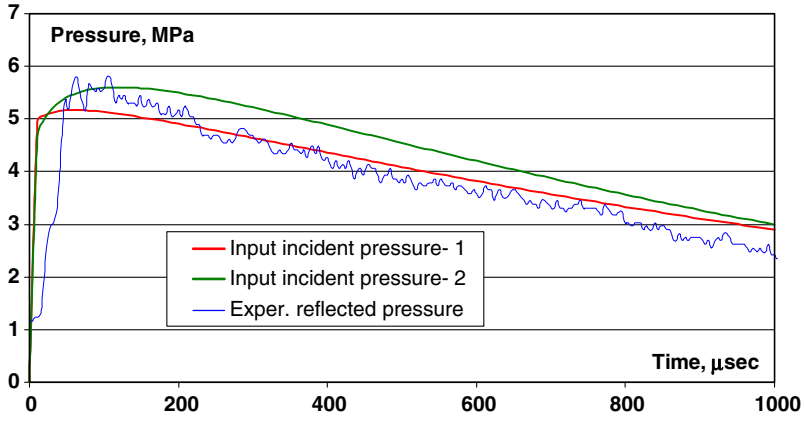

Fig. 21. Experimental pressure history measured by reflected pressure gauge (blue line) and two incident pressure histories used as input for the analysis (normalized here for uniform distribution case); pressure 1 is defined by Eqs. 9 and 10 and pressure 2 by (9)–(21). (For interpretation of the references to colour in this figure legend, the reader is referred to the web version of this article.)

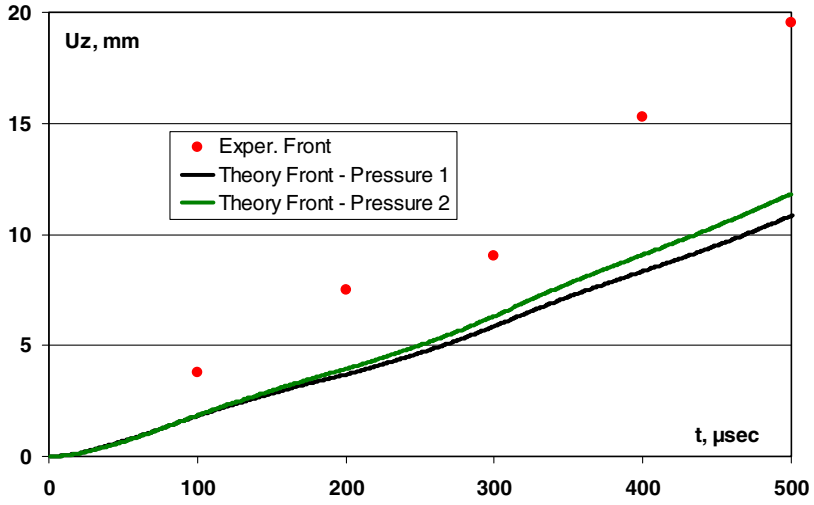

Fig. 22. Experimental points for sandwich 1 front face deflection and two theoretical curves corresponding to the incident pressure histories Eqs. 9 and 10 – pressure 1 and (9)–(21) – pressure 2.

multi-layer preforms combining both aforementioned fabrics. However, this effect cannot be large. The other possible reason of lowering elastic properties of composite skins might be insufficient resin penetration between the yarns and/or into the yarns. This is purely speculative at this point. The possibility of insufficient wetting and/or filling the skin fabrics during pultrusion requires special investigation into the utilized pultrusion process, as well as direct mechanical characterization of the produced composite skins. Finally, one can argue that severe in-plane fiber damage due to stitching may have occurred, which is possible. However, if this is true, it contradicts the observation that when stitching density is increased, the agreement between theoretical and experimental results gets better.

(4) It is possible that the measured experimental deflection values (red[3] points in Figs. 14–19) have a small error. However, the error margins are not as large as the discrepancies seen in Figs. 14–19. It is to be noted that the time scale on the high-speed camera and the time scale of the oscilloscope recording the pressure data are not the same during the experiments. After the experiments are done, the time scales are synchronized by calculating the time taken for the reflected pressure to reach the sensor and shifting the time scale of high-speed images accordingly. In spite of best estimations, there might be some time lag (estimated in the order of 20–40 μs) in the actual "time zero" of these images (deflection response) when compared to "time zero" of the pressure sensor. It is not believed that this effect may a major cause for the discrepancies under discussion, as seen in subsequent discussion on varying pressure profile.

(5) A good correspondence between the incident pressure history assumed in the analysis (it was defined by Eqs. (9) and (10)) and experimental pressure acting on the test sample in shock tube have to be carefully verified. For this purpose, we compared the two pressure histories in Fig. 21 and added another one, which was also defined by Eq. (9), but with different numerical parameters:

$$P_0 = 5.6\ \text{MPa}, \quad n = 0.12, \quad B = 0.001\ \mu\text{s}^{-1} \tag{21}$$

These parameters provide the peak pressure value $P(t_0) = 5.6$ MPa, which is reached at $t_0 = 120$ μs time instant. As before, the P_0 value in (21) corresponds to uniform distribution of the incident pressure; due to a half-sine wave distribution

[3] For interpretation of the references to colour in this figure legend, the reader is referred to the web version of this article.

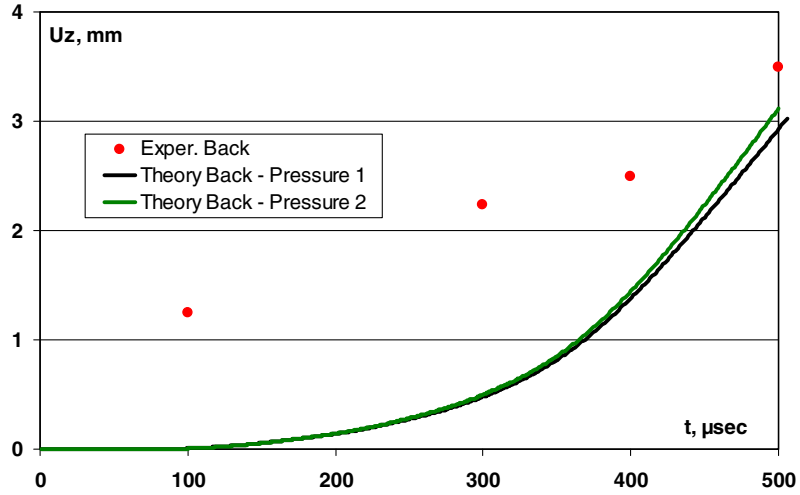

Fig. 23. Experimental points for sandwich 1 back face deflection and two theoretical curves corresponding to the incident pressure histories 9 and 10 – pressure 1 and (9)–(21) – pressure 2.

was assumed in the analysis runs, the respective load amplitude was multiplied by factor $(\pi/2)^2$ in order to keep equivalency between the integral pressure values. It is also worth noting that control analysis was performed with uniform pressure distribution and showed hardly distinguishable results for deflection from the ones obtained in the half-sine pressure distribution case.While the pressure 1 approximation is overall closer to the experimental curve, the pressure 2 approximation it much better near the peak. Most importantly, the latter one is not under suspicion that it below the experimental pressure history. Numerical results for the two pressure histories are mutually compared, and also compared to experimental data for sandwich 1, in Figs. 22 and 23. The foam core properties are taken as defined by Eq. (14).Comparison of theoretical and experimental results for the front face in Fig. 22 shows some increase in transient deflection values for pressure 2 case, which one could expect. However, that increase is much lower than the discrepancy between both theoretical curves on one side, and experimental data points on the other. This conclusion is even stronger when comparing results for the back face in Fig. 23. So, varying the pressure pulse history makes some quantitative effect, but does not help to understand where the major discrepancy is coming from.

(6) After analyzing all the above possible factors, we come to the conclusion that none of them individually, or all of them together, would be able to cause the observed discrepancies between theoretical and experimental results. Intuition tells that there is some more fundamental difference between the actual specimen loading conditions in the shock tube, and the respective boundary value problem formulation. One possible difference of this kind is that experimental pressure curve shown in Fig. 21 it not an incident pressure measured on each tested specimen. Rather, this is so-called "reflected pressure" history which is measured by a transient pressure gauge mounted on the tube inner surface at some small distance from the sample, see [14] for details.

Most importantly, the experimental reflected pressure history was recorded in special "calibration tests" conducted with a rigid steel plate used in place of actual test specimens. Obviously, the composite sandwich specimens studied here are very far below steel plate in their transverse stiffness, so the actual incident pressure acting on the sandwich samples might be very different from the reflected pressure history which was approximated and used in the analysis. By exaggerating the case, one may bring an example that if a sheet of paper is standing at the end of shock tube, the reflected pressure will not be even seen by the sensor. Another argument to support this hypothesis is that, if it proves correct, the aforementioned effect of getting the obtained theoretical and experimental results closer and closer agreement with increasing transverse stiffness of the sandwich, will be readily explained. Special experimental study is needed to clarify this issue.

7. Conclusions

Experimental methodology of material testing in a shock tube, developed by this group of authors was applied in this paper to three samples of unstitched, intermediately stitched and densely stitched TRANSONITE® sandwich panels.

The first experimental study of its kind reported here was conducted with the use of shock tube, where simply supported sandwich panel is exposed to a high intensity transient pressure load. First group of results include real time images of the deflection and progressive damage of the skins and core taken by high-speed camera. These results revealed quite a dramatic difference between the transient responses of sandwich panels with unstitched foam core on one side and stitched foam core on the other. In the former case, the front skin (exposed to shock pressure) deflects almost independently of the back skin, the load transfer within sandwich construction is not accomplished and, as the result, test specimen fails at an early stage of deformation process. Contrary to that, in both cases of stitched foam cores, the deformation mode is more like in sync bending of both skins, with much smaller difference in their dynamic deflections. This evidences that the transient load transfer through the core is much better with the stitching and, as the result, the imparted damage is substantially reduced. The maximum deflection of sandwich panel with highest stitching density used here did not even reach one thickness of the front skin.

The second group of experimental results was obtained by visual post-mortem examination of the shock loaded panels, including residual deformation and damage evaluation. These results provided additional important insight into the effect of 3-D woven skin and unstitched/stitched core construction on the performance of composite sandwiches exposed to shock wave loading. In general, the sandwich composites with through-thickness stitching

Please cite this article in press as: Tekalur SA et al., Shock loading response of sandwich panels with 3-D woven E-glass composite skins ..., Compos Sci Technol (2008), doi:10.1016/j.compscitech.2008.03.017

show delayed damage initiation, increased damage tolerance against high intensity stress wave propagation, and only minimal visually recognizable residual damage. Also worth noting that the dominating damage type is different for unstitched and stitched sandwiches, and increasing stitching density may further alter it.

Overall, as demonstrated in this experimental study, by combining 3-D woven preforms as the skin reinforcement and through-thickness stitching of such preforms together with foam core, one can get a variety of light-weight sandwich constructions, and there are quite obvious ways to further increase their shock wave resistance and damage tolerance. In order to accomplish this goal, it will be necessary to support future experimental studies by theoretical analysis which is capable of predicting the transient 3-D displacement, strain and stress fields along with damage and failure initiation and progression processes in composite sandwich structures.

An important first step in this direction was made in the present paper – probably, for the first time ever a direct comparison between theoretical and experimental results has been performed for this kind of complex composite sandwich structures exposed to shock wave loading. Though the results of such comparison are not always as close as desired, they are also very encouraging. Of a particular interest is the trend that when stitching density is increased, the theoretical and experimental results get closer. Several possible causes for observed discrepancies between theoretical and experimental results have been identified and discussed in the paper.

This work demonstrates that further comprehensive and insightful experimental and theoretical studies are needed to achieve sufficient understanding of a very complex transient behavior of composite sandwiches under shock wave loading.

Acknowledgements

The authors acknowledge the financial support from the Office of Naval Research under Grant No. N000140410268. The authors are thankful to Mrs. Grey Chapman of Martin Marietta Composites and Dr. Mansour Mohamed of 3TEX for supplying sandwich materials used in this study and helpful discussion of some aspects of their manufacturing and properties. Special thanks to Dr. Dmitri Mungalov of 3TEX who provided compression test data for the sandwiches and assisted in the illustration preparation for the paper.

References

[1] Vinson JR. The behavior of sandwich structures of isotropic and composite materials. Lancaster, PA: Technomic; 1999.
[2] Davies JM. Lightweight sandwich construction. Oxford: Wiley–Blackwell; 2001.
[3] Vautrin A, editor. Mechanics of sandwich structures. Springer; 1998.
[4] Tagarielli VL, Deshpande VS, Fleck NA. The dynamic response of composite sandwich beams to transverse impact. Int J Solids Struct 2007;44(7–8):2442–57.
[5] Shukla A, Tekalur SA, Rousseau C, Bogdanovich A, LeBlanc J. Performance of 3-D woven composites under shock loading. In: CD-ROM proceedings of the 16th international conference on composite materials (ICCM-16), Kyoto, Japan, July 8–13, 2007.
[6] Vaidya UK, Nelson S, Sinn B, Mathew B. Processing and high strain rate impact response of multi-functional sandwich composites. Compos Struct 2001;52:429–40.
[7] Rice MC, Fleischer CA, Zupan M. Study on the collapse of pin-reinforced foam sandwich cores. Exp Mech 2006;46(2):197–204.
[8] Baker WE, Cox PA, Westine PS, Kulesz JJ, Strehlow RA. Explosion hazards and evaluation. New York: Elsevier Scientific; 1983.
[9] Kinney GF, Graham KJ. Explosive shocks in air. New York: Springer–Verlag; 1985.
[10] Zukas JA, Walters WP. Explosive effects and applications. New York: Springer; 1998.
[11] Structures to resist the effects of accidental explosions. Technical manual for Army TM 5-1300, Navy NAVFAC P-397, and Air Force AFR 88-22, November 1990.
[12] Design of blast resistant buildings in petrochemical facilities. Document prepared by the Task Committee on blast resistant design of the Petrochemical Committee of the Energy Division of the ASCE, 1997.
[13] Design and analysis of hardened structures to conventional weapons effects. Technical manual for Army TM 5-855-1, Air Force AFPAM 32-1147(I), Navy NAVFAC P-1080, and Defense Special Weapons Agency DAHSCWEMAN-97, August 1998.
[14] LeBlanc J, Shukla A, Rousseau C, Bogdanovich A. Shock loading of three-dimensional woven composite materials. Compos Struct 2007;79(3):344–55.
[15] Bogdanovich AE. Three-dimensional variational theory of laminated composite plates and its implementation with Bernstein basis functions. Computer Meth Appl Mech Eng 2000;185(2–4):279–304.
[16] Bogdanovich AE, Yushanov SP. Three-dimensional variational impact contact analysis of composite bars and plates. Compos A: Appl Sci Manuf 2000;31A(8):795–814.
[17] Bogdanovich AE, Yushanov SP. Progressive failure analysis of adhesive bonded joints with laminated composite adherends. J Reinforced Plastics Compos 1999;18(18):1689–707.
[18] Bogdanovich AE. Multi-scale modeling, stress and failure analyses of 3-D woven composites. J Mater Sci 2006;41(20):6547–90.
[19] Bogdanovich AE, Yushanov SP. 3-D blast performance analysis of concrete walls with layered composite protection/retrofit. In: Proceedings of the american society for composites, fourteenth technical conference, September Dayton, OH, 1999, p. 151–60.
[20] Bogdanovich AE. Three-dimensional blast response simulation of layered composite armor panels. In: Reddy JN, Chandra N, editors. CD proceedings of the 3rd international conference on structural stability and dynamics (ICSSD), Kissimmee, FL, June 19–22, 2005.
[21] Mohamed MH, Bogdanovich AE, Dickinson LC, Singletary JN, Lienhart RB. A new generation of 3D woven fabric preforms an composites. SAMPE J 2001;37(3):8–17.
[22] Mohamed MH, Bogdanovich AE, Coffelt RA, Schartow R, Stobbe D. Manufacturing, performance and applications of 3-D orthogonal woven fabrics. In: CD proceedings of the textile institute 84th annual world conference, Raleigh, NC, March 22–25, 2005.
[23] Bogdanovich AE. Advancements in manufacturing and applications of 3D woven preforms and composites. In: CD-ROM proceedings of the 16th international conference on composite materials (ICCM-16), Kyoto, Japan, July 8–13, 2007.
[24] Bogdanovich AE. Multiscale predictive analysis of 3-D woven composites. In: CD proceedings of the 35th international SAMPE technical conference, vol. 35, Dayton, OH, September 28–October 2, 2003.

Please cite this article in press as: Tekalur SA et al., Shock loading response of sandwich panels with 3-D woven E-glass composite skins ..., Compos Sci Technol (2008), doi:10.1016/j.compscitech.2008.03.017